energies

MDPI

Article

A Non-Linear Flow Model for Porous Media Based on Conformable Derivative Approach

Gang Lei [1], Nai Cao [2], Di Liu [3] and Huijie Wang [4,*]

1 College Petroleum of Engineering & Geoscience, King Fahd University of Petroleum and Minerals, Dhahran 31261, Saudi Arabia; gang.lei@kfupm.edu.sa
2 College of Petroleum Engineering, China University of Petroleum, Beijing 102249, China; caonai99@gmail.com
3 School of Mechanics and Civil Engineering, China University of Mining and Technology, Beijing 100083, China; liudi@student.cumtb.edu.cn
4 College of Engineering, Peking University, Beijing 100871, China
* Correspondence: jie.wh@pku.edu.cn; Tel.: +86-010-6276-0875

Received: 11 September 2018; Accepted: 29 October 2018; Published: 1 November 2018

Abstract: Prediction of the non-linear flow in porous media is still a major scientific and engineering challenge, despite major technological advances in both theoretical and computational thermodynamics in the past two decades. Specifically, essential controls on non-linear flow in porous media are not yet definitive. The principal aim of this paper is to develop a meaningful and reasonable quantitative model that manifests the most important fundamental controls on low velocity non-linear flow. By coupling a new derivative with fractional order, referred to conformable derivative, Swartzendruber equation and modified Hertzian contact theory as well as fractal geometry theory, a flow velocity model for porous media is proposed to improve the modeling of Non-linear flow in porous media. Predictions using the proposed model agree well with available experimental data. Salient results presented here include (1) the flow velocity decreases as effective stress increases; (2) rock types of "softer" mechanical properties may exhibit lower flow velocity; (3) flow velocity increases with the rougher pore surfaces and rock elastic modulus. In general, the proposed model illustrates mechanisms that affect non-linear flow behavior in porous media.

Keywords: porous media; non-linear flow; conformable derivative; fractal

1. Introduction

Ever since Henry Darcy (1865) developed his famous linear flow model (the classical Darcy's law), based on a series of sand pack experiments, the linear flow through porous media has drawn tremendous attention in various scientific and engineering field [1,2]. However, it's a common phenomenon that experiments on low velocity flow in tight porous media, deviate from the Darcy's law and the flow velocity is lower than that predicted from Darcy's law. As stated in the literature, the existence of low velocity non-Darcy flow (or low velocity non-linear flow) in tight porous media (e.g., shale gas/oil reservoirs, coalbed, or tight gas/oil reservoirs) is due to the interaction forces between the fluid and tight pores [3,4]. Many scholars have documented that, there existed threshold Reynolds number or pressure gradient, which could be used to well describe low velocity non-linear flow [5–7]. And they concluded that there is no flow in tight porous media when the pressure gradient is beyond the certain value (i.e., threshold pressure gradient). However, Li provided contradictory evidence for the threshold pressure gradient [8]. He suggested that the threshold pressure gradient measured in labs can be probably ascribed to the difficulty in measuring lower flow velocity, and the false phenomenon of the existence of threshold pressure gradient is strengthened by the skin effect.

Until now, appropriate non-linear model for fluid flow through tight porous media remains unclear, though some more formulas have been established to describe the non-linear flow, such as power function model [9], exponential function model [10], incomplete Gamma function model [11,12] and fractional derivative approach [13–15]. As stated in the literature, in some extent, these models above are suitable for the description of non-linear flow in porous media with lower permeability [9–14]. Most recently, Yang [14] and Zhou [15] also suggested that the conformable derivative approach is suitable for the describing non-linear flow in low-permeability porous media. However, these models above never took effective stress into account. It is reported that the porous media will be compressed as the effective stress increases, causing fluid flow behavior in porous media to be strongly stress-dependent [16–24].

As implied by this brief literature review, we suggest that the characteristic behavior of non-linear flow is still not definitively determined. Therefore, a major goal of this research was to develop an analytical model in a closed form for the description of low velocity non-linear flow. The specific objectives of this work were: (1) to establish a reasonable quantitative model to quantify the essential controls on non-linear flow; (2) to verify the model with available experimental data. Compared with the previous models, our model takes into account more factors, including the influence of the effective stress and the microstructural parameters of the pore space. The proposed models can reveal more mechanisms that affect the low velocity non-linear flow in porous media.

2. Mathematical Model

In this section, the analytical low velocity non-linear flow model for porous media is detailed. The conformable derivative is used to develop the Swartzendruber model for description of low velocity non-linear flow in pores, the fractal geometry theory and modified Hertzian contact theory are used to describe the complex pore structure of porous media under stress condition.

2.1. Model Assumptions

The following assumptions are made to simplify the flow system:

1. The porous media is composed by a bundle of capillary bundles and a single capillary with the equivalent radius r is made up of a packing of equivalent spherical grains.
2. The interspaces in porous media have fractal characteristics.
3. The single phase flow is under isothermal and stress condition, which is fully developed and at steady state.
4. The deformation of porous media obeys Hertzian contact theory.
5. During the flow, the fluid has constant viscosity and density.

2.2. Conformable Derivative Approach to Swartzendruber Equation

As suggested by decades of literature, the Swartzendruber equation can well describe the non-Darcian flow in tight porous media with low permeability [13,14]. Based on the Swartzendruber equation, the following equation can be written as:

$$\frac{du}{di} = \frac{K\rho g}{\mu}\left(1 - e^{-\frac{i}{I}}\right), \tag{1}$$

where u is the flow velocity in the cross section; K is the permeability of porous media; μ is fluid viscosity; ρ is fluid density, g is the gravitational acceleration, i and I represent hydraulic gradient and threshold hydraulic gradient, respectively. According to Equation (1), the flow velocity in a single capillary with radius r can be written as:

$$\frac{du}{di} = \frac{r^2\rho g}{8\mu}\left(1 - e^{-\frac{i}{I}}\right), \tag{2}$$

where r is the radius of the capillary.

As the linear operator does not inherit all the operational behaviors from the typical first derivative, the Swartzendruber equation fails to capture the full range of non-Darcy flow behavior in porous media [13–15]. Fortunately, as a well-behaved and efficient method, conformable derivative approach with real order can be applied to address this problem. The conformable derivative of the flow velocity $u(i)$: $[0, \infty) \to \mathrm{R}$ for all $i > 0$ with order $\alpha \in (0, 1]$ can be defined by [10]:

$$T_\alpha u(i) = \lim_{\varepsilon \to 0} \frac{u\left(i + \varepsilon i^{1-\alpha}\right) - u(i)}{\varepsilon}, \tag{3a}$$

and the conformable derivative at 0 is given by $(T_\alpha u)(0) = \lim_{i \to 0} (T_\alpha u)(i)$.

As stated in the literature [10,14,25], the relationship between the conformable derivative and the first derivative can be written as:

$$T_\alpha u(i) = i^{1-\alpha} \frac{du(i)}{di}. \tag{3b}$$

Equation (3b) shows that the conformable derivative coincides with the classical first derivative with a given differential order $\alpha = 1$, which means the conformable derivative is a modification of classical derivative in direction and magnitude [25–27]. As stated in the literature [25–27], the physical interpretation of the conformable derivative is a modification of classical derivative indirection and magnitude. Replacing the first order derivative in Equation (2) with conformable derivative, the Swartzendruber equation can be rewritten as:

$$T_\alpha u(i) = \frac{r^2 \rho g}{8\mu} \left(1 - e^{-\frac{i}{I}}\right). \tag{4}$$

By solving Equation (4) with Laplace transform and inverse Laplace transform, the flow velocity in the cross section can be determined as:

$$u(i) = \frac{r^2 \rho g}{8\mu} \frac{i^\alpha}{\alpha} \left[1 - {}_1F_1\left(\alpha; \alpha + 1; -\frac{i}{I}\right)\right], \tag{5}$$

where ${}_1F_1\left(\alpha; \alpha + 1; -\frac{i}{I}\right) = \sum_{j=0}^{\infty} \frac{\alpha^{(j)}}{(\alpha+1)^{(j)}} \frac{(-i/I)^j}{j!}$ is the Kummer confluent hypergeometric function [23].

Based on Equation (5), the flow rate q in the cross section can be written as:

$$q = \frac{\pi r^4 \rho g}{8\mu} \frac{i^\alpha}{\alpha} \left[1 - {}_1F_1\left(\alpha; \alpha + 1; -\frac{i}{I}\right)\right], \tag{6}$$

where q is the flow rate in the capillary with the radius r.

2.3. Non-Linear Flow Model

The fractal theory is used to develop the non-linear flow model for tight porous media. Based on fractal theory and modified Hertzian contact theory described in detail in [28,29], the total volumetric flow rate Q in the cross section under stress condition can be calculated by integrating the flow rate over the radius ranging from the minimum radius $r_{\min}$ to the maximum porous radius $r_{\max}$ [28–33]:

$$Q = N \int_{r_{\min}}^{r_{\max}} q f dr, \tag{7}$$

with:

$$\begin{cases} N = (r_{\max}/r_{\min})^{D_f}; f(r) = D_f r_{\min}^{D_f} r^{-(D_f+1)}, \\ r = r_0 \left\{ 1 - 4 \left[\dfrac{3\pi(1-v^2)p_{\text{eff}}}{4E} \right]^{\beta} \right\}, \\ r_{\min} = r_{\min 0} \left\{ 1 - 4 \left[\dfrac{3\pi(1-v^2)p_{\text{eff}}}{4E} \right]^{\beta} \right\}, \\ r_{\max} = r_{\max 0} \left\{ 1 - 4 \left[\dfrac{3\pi(1-v^2)p_{\text{eff}}}{4E} \right]^{\beta} \right\}. \end{cases} \tag{8}$$

In Equation (8), N is the number of pores; r_0 and r are the initial pore radius and pore radius under stress condition, respectively. f is the probability density function for pore size distribution; β is the power law index which is related to the structure of pore surface. $r_{\max 0}$ and $r_{\min 0}$ are the maximum and minimum pore radius of porous media at zero stress, respectively. $r_{\max}$ and $r_{\min}$ are the stress-dependent maximum and the stress-dependent minimum pore radius of porous media, respectively. p_{eff} is the effective stress, E is rock elastic modulus and v is rock Poisson's ratio. D_f is the fractal dimension for pore size distribution which can be determined as [32,33]:

$$\begin{cases} D_f = 2 - \dfrac{(2-D_{f0})r_{\max 0}}{(3-D_{f0})r_{\max} - (2-D_{f0})r_{\max 0}}, \\ D_{f0} = 2 - \dfrac{\ln \varphi_0}{\ln(r_{\min 0}/r_{\max 0})}, \end{cases} \tag{9}$$

where φ_0 is the initial porosity of the porous media, and D_{f0} is the fractal dimension for pore size distribution at zero stress.

Substituting Equations (6), (8) and (9) into Equation (7), the flow rate can be rewritten as:

$$Q = \frac{\pi \rho g D_f r_{\max}^{D_f}}{8\mu} \frac{i^{\alpha}}{\alpha} \left[1 - {}_1F_1\left(\alpha; \alpha+1; -\frac{i}{I} \right) \right] \frac{r_{\max}^{4-D_f} - r_{\min}^{4-D_f}}{4-D_f}. \tag{10}$$

As stated in the literature [32–35], the cross sectional area of a unit cell A can be expressed as:

$$A = \frac{\pi D_f r_{\max}^2 \left[1 - (r_{\min}/r_{\max})^{2-D_f} \right]}{(2-D_f)(r_{\min}/r_{\max})^{2-D_f}}. \tag{11}$$

Then, based on Equations (10) and (11), the average flow velocity u_{av} can be written as:

$$u_{\text{av}} = \frac{Q}{A} = \frac{\rho g \varphi i^{\alpha} (2-D_f)(r_{\max}^2 - \varphi r_{\min}^2)}{8\alpha\mu(1-\varphi)(4-D_f)} \left[1 - {}_1F_1\left(\alpha; \alpha+1; -\frac{i}{I} \right) \right] \tag{12}$$

It is evident that the flow rate (or average flow velocity) is the function of pore structural parameters, power law index, rock elastic modulus, effective stress, and differential order α as well as hydraulic gradient and threshold hydraulic gradient.

3. Results and Discussion

This section aims at studying the novel analytical models in detail. In the following, we first compare our results with those from experimental data. Then, in order to analyze essential controls on non-linear flow in tight porous media, the effects of relevant parameters on average flow velocity are studied in detail.

The availability of the proposed model Equation (12) depends on its ability to adequately fit experimental data [15]. To verify our quantitative model, the measured average flow velocity versus hydraulic gradient relationship in [36] and that predicted by our proposed model are compared

(Figure 1). In the experiment of Prakash K. et al. [36], the flow velocity tests were conducted on soils at an effective consolidation stress of 6.25 kPa during loading process. In our proposed model, the initial porosity of rock is 15%, the rock elastic modulus is 45 GPa, the rock Poisson's ratio is 0.23 and power law index is 3/4. Furthermore, to ensure the effective consolidation stress is 6.25 kPa, the effective stress assigned is 6.25 kPa. The values of other parameters (e.g., r_{max0}, r_{min0}, differential order α and threshold hydraulic gradient I) are listed in the Figure 1. Results displayed in Figure 1 suggest that the proposed model calculated relationship between average flow velocity and hydraulic gradient is in good agreement with that determined by experimental data [36]. Results (Figure 1) also suggest a definitive positive correlation between the average flow velocity and hydraulic gradient.

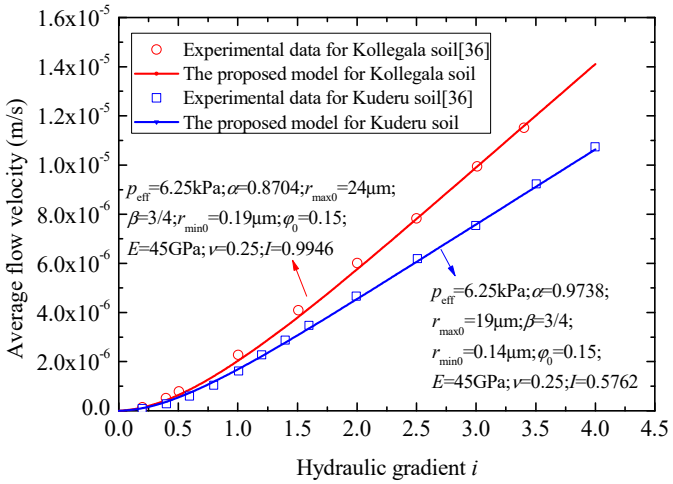

Figure 1. A comparison between the experimental data [36], and results of the proposed model.

Figure 2 provides a comparison of the relationship between average flow velocity and hydraulic gradient predicted by the proposed model with experimental data of [37]. In the experiment of Zhang et al. [37], the permeability tests were conducted on gap-graded sands (e.g., sand A, sand B and sand C) to determine the critical hydraulic gradient of piping in sands. Sand A, sand B and sand C were prepared by mixing a coarse sand with particle size of 3–5 mm and a fine sand with particle size of 0.25–0.50 mm at various ratios of 4:1, 5:1 and 6:1 respectively.

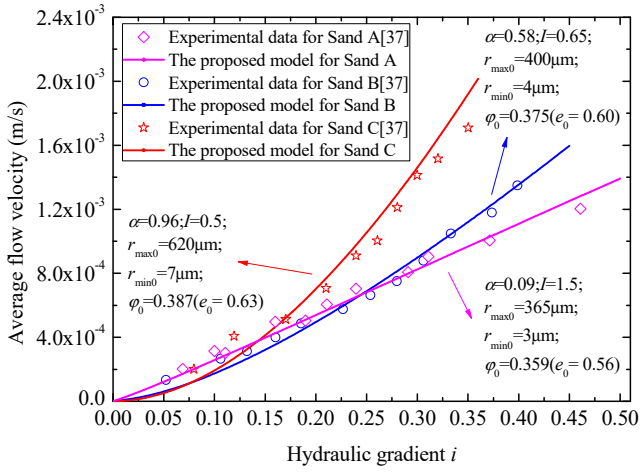

Figure 2. A comparison between the experimental data [37], and results of the proposed model.

For sand A, the hydraulic conductivity and void ratio are 2.6 × 10^{-3} m/s and 0.56 respectively. The hydraulic conductivity and void ratio of sand B are 3.6 × 10^{-3} m/s and 0.60 respectively. In addition, for sand C, the hydraulic conductivity and void ratio are 4.0 × 10^{-3} m/s and 0.63

respectively. To ensure the porous media simulated in the proposed model exhibits the same physical properties as the porous media tested in the experiments of [37], the initial void ratio e_0 and initial porosity φ_0 (i.e., $\varphi_0 = e_0/(1 + e_0)$) applied in the proposed model are the same with that of the sands in the experiments and the effective stress assigned is 0 MPa. The values of other parameters (e.g., r_{max0}, r_{min0}, differential order α and threshold hydraulic gradient I) are listed in the Figure 2. It can be seen from Figure 2 that our predicted values agree well with the corresponding experimental data [37].

As the average flow velocity is related to the threshold hydraulic gradient, differential order α, effective stress, rock elastic modulus, power law index, pore structural parameters, and the hydraulic gradient. We will then study the effects of these relevant parameters (e.g., threshold hydraulic gradient, differential order α, effective stress, rock elastic modulus, power law index and initial porosity) on average flow velocity in detail to analyze essential controls on non-linear flow in tight porous media. We plotted average flow velocity vs. hydraulic gradient with different threshold hydraulic gradient I and different differential order α (Figure 3a,b).

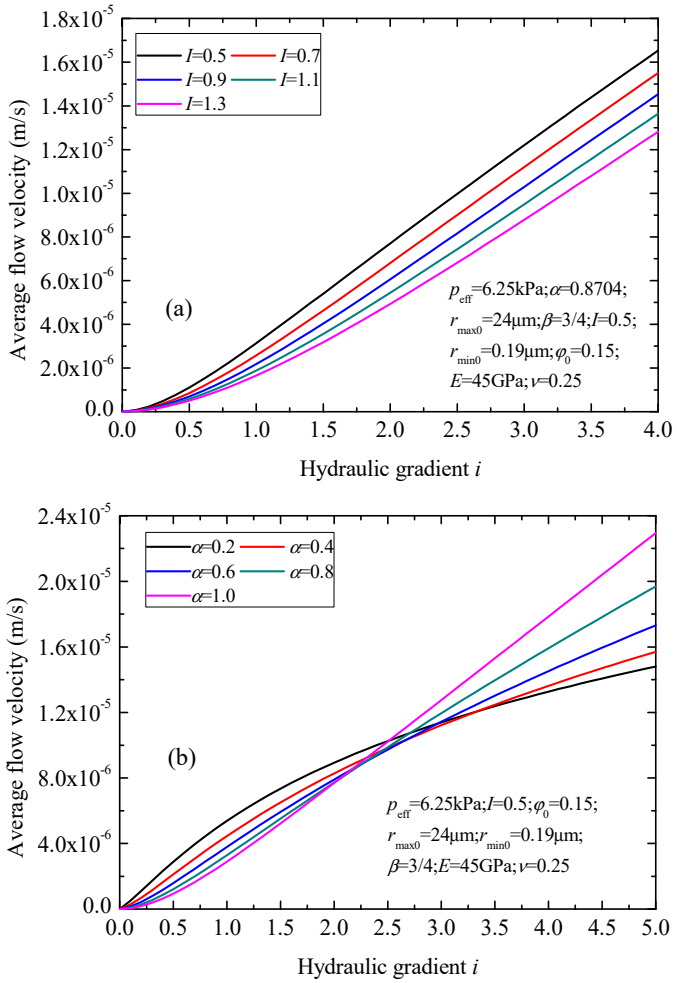

Figure 3. The average flow velocity curves: (**a**) for different threshold hydraulic gradient I; (**b**) for different differential order α.

The parameters assigned in the proposed model were listed in the Figure 3. As suggested by the results (Figure 3a), average flow velocity decreases as threshold hydraulic gradient increases. In addition, Figure 3b shows that larger different differential order leads to smaller average flow velocity with smaller hydraulic gradient, however, on the contrary, when the hydraulic gradient increases to a certain value, average flow velocity increases as differential order increases.

Figure 4 illustrates the average flow velocity vs. hydraulic gradient with different effective stress. The parameters assigned in the proposed model were listed in the Figure 4. As suggested by the results (Figure 4), average flow velocity decreases as effective stress increases. This may be attributed to the decrease of pore radius which is resulted from the pore compaction. Therefore, fluid flow behavior in tight porous media is strongly stress-dependent.

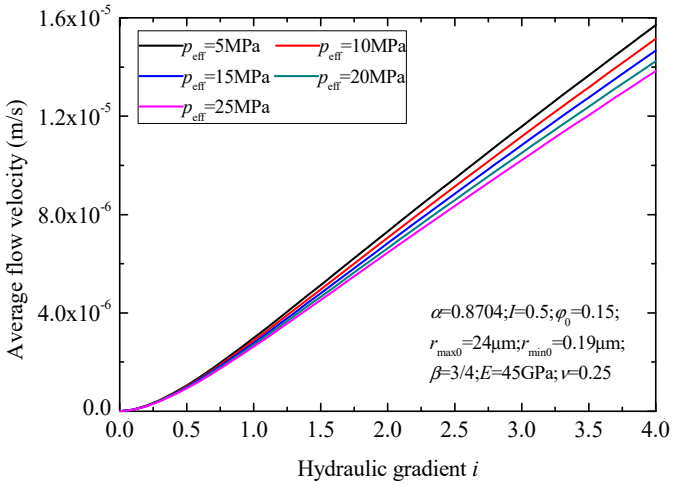

Figure 4. The average flow velocity curves versus hydraulic gradient with different effective stress.

Plotting average flow velocity vs. hydraulic gradient with different rock elastic modulus, power law index and initial porosity (Figure 5) was also useful. For the necessary calculations, the parameters assigned in the proposed model were listed in the Figure 5. As suggested by the results (Figure 5a), the average flow velocity increases as rock elastic modulus increases. We interpret this result to indicate that the larger rock elastic modulus decreases the contact surface radius of a given particle, leading to reduced pore volume compressibility and larger hydraulic conductivity. Therefore, rock types of "soft" lithology can yield lower flow velocity. As suggested by the results (Figure 5b), the average flow velocity increases as power law index increases. Correspondingly, we suggest that the larger power law index β implies rougher pore surfaces, leading to only a limited number of pores being compressed and the larger hydraulic conductivity. Figure 5c shows the average flow velocity decreases as rock initial porosity decreases, which is expected. Correspondingly, we suggest that the smaller initial porosity implies narrower pore radius, leading to the smaller hydraulic conductivity.

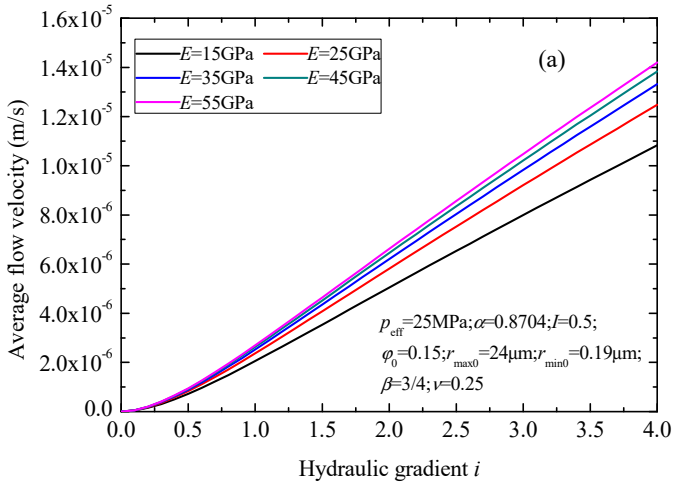

Figure 5. *Cont.*

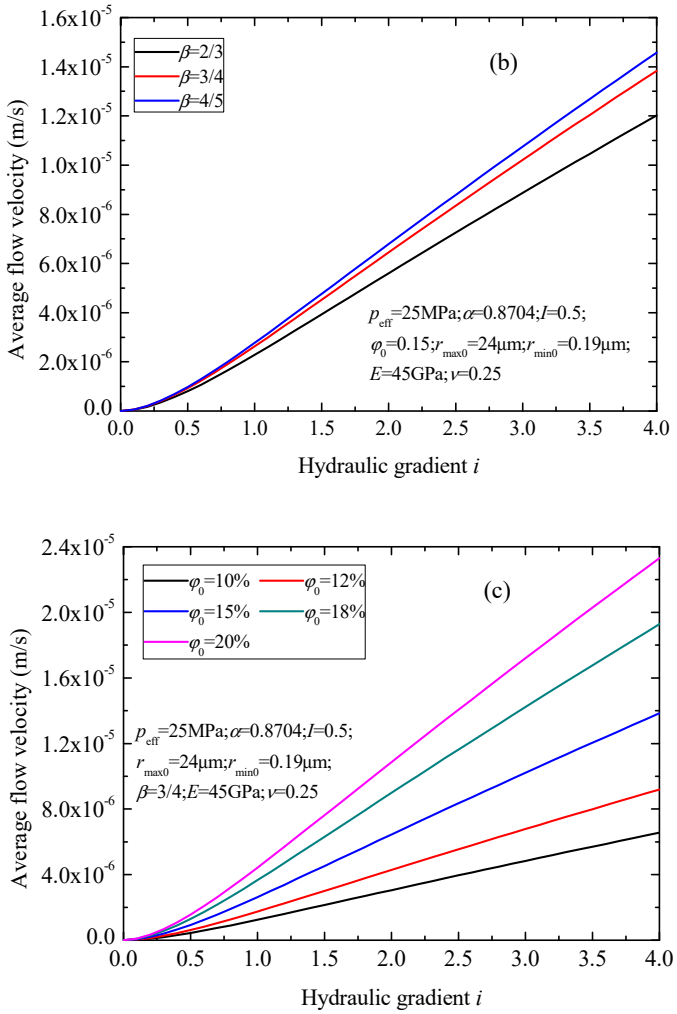

Figure 5. The average flow velocity curves: (**a**) for different rock elastic modulus; (**b**) for different power law index; (**c**) for different initial porosity.

4. Conclusions

In this study, we developed a novel non-linear flow model for tight porous media. The model is based on Swartzendruber equation and conformable derivative approach and as well as the modified Hertzian contact theory and fractal geometry, and allowed us to analyze essential controls on non-linear flow in tight porous media. An advantage of this model is that it lacks empirical constants, and, more importantly, every parameter in the model has specific physical significance. Predictions from the proposed analytical model exhibit similar variation trends as experimental data, suggesting validity of the model to predict the average flow velocity. Moreover, we analyzed resulting model predictions in detail, to confirm the model's robustness in this context. Results of the new model show the following salient conclusions:

1. The proposed models indicate that average flow velocity in tight porous media is a function of microstructural parameters of the pore space, rock lithology and differential order α as well as hydraulic gradient and threshold hydraulic gradient.
2. The parametric study reveals that average flow velocity increases with the rougher pore surfaces and rock elastic modulus, and decreases with increasing effective stress. "Softer" rock lithology may yield lower average flow velocity.
3. This non-linear model presented here considers microstructural parameters of pore space and rock lithology; we have shown that its forecasted values are robust, at least compared to experimental

data, and thus may be useful for performance predictions of non-linear flow behavior in tight porous media. Results also reveal more information about the details of specific parameters (and therefore mechanisms) that affect non-linear flow behavior in porous media. The new model presented in this work can be used to depict the non-linear flow in tight porous media, and may provide meaningful applications for design and development of tight reservoirs. In addition, as the model takes effective stress into account, it is also useful for performance predictions of the coupled flow deformation behavior (stress sensitivity) in tight porous media.

Author Contributions: Conceptualization, G.L.; Funding acquisition, H.W.; Investigation, N.C. and D.L.; Methodology, G.L.; Project administration, H.W.; Visualization, N.C.; Writing—original draft, G.L.; Writing—review & editing, H.W.

Funding: This research was funded by the State Major Science and Technology Special Project of China during the 13th Five-Year Plan (grant number: 2016ZX05025-003-007 and 2016ZX05014004-006). Appreciation and thanks are given to the organizations for their finical funding herein.

Conflicts of Interest: The authors declare no conflicts of interest.

Nomenclature

Latin symbols	
A	Cross sectional area of a unit cell, μm^2
D_{f0}	Initial pore area fractal dimension at zero stress, dimensionless
D_f	Pore area fractal dimension, dimensionless
e_0	Initial void ratio of porous media, dimensionless
E	Rock elastic modulus of porous media, GPa
f	Probability density function for pore size distribution, dimensionless
${}_1F_1$	Kummer confluent hypergeometric function
g	Gravitational acceleration, N/kg
K	Absolute permeability of porous media, μm^2
i	Hydraulic gradient, dimensionless
I	Threshold hydraulic gradient, dimensionless
N	Number of pores of a unit cell, dimensionless
p_{eff}	Effective stress, MPa
q	Flow rate in the cross section, m^3/s
Q	Total volumetric flow rate in the cross section under stress condition, m^3/s
r_0	Initial equivalent pore radius of capillary at zero stress, μm
r	Equivalent pore radius of capillary under effective stress, μm
u	Flow velocity in the cross section, m/s
u_{av}	Average flow velocity, m/s
Greek symbols	
α	Differential order
β	Power law index, dimensionless
μ	Fluid viscosity, mPa·s
ρ	Fluid density, kg/m^3
φ_0	Initial porosity of porous media, dimensionless
φ	Porosity under effective stress, dimensionless
ν	Poisson's ratio, dimensionless
Subscript	
av	Average
eff	Effective
max	maximum values
max0	Initial maximum values at zero stress
min	minimum values
min0	Initial minimum values at zero stress

References

1. Freeze, R.A.; Cherry, J.A. *Groundwater*; Prentice-Hall: Upper Saddle River, NJ, USA, 1979.
2. Zhang, J.; Xu, Q.; Chen, Z. Seepage analysis based on the unified unsaturated soil theory. *Mech. Res. Commun.* **2001**, *28*, 107–112. [CrossRef]
3. Xu, C.; Kang, Y.; Chen, F.; You, Z. Analytical model of plugging zone strength for drill-in fluid loss control and formation damage prevention in fractured tight reservoir. *J. Pet. Sci. Eng.* **2017**, *149*, 686–700. [CrossRef]
4. Cai, J.; Lin, D.; Singh, H.; Wei, W.; Zhou, S. Shale gas transport model in 3D fractal porous media with variable pore sizes. *Mar. Geol.* **2018**, *98*, 437–447. [CrossRef]
5. Thomas, L.K.; Katz, D.L.; Tek, M.R. Threshold pressure phenomena in porous media. *Soc. Petrol. Eng. J.* **1968**, *8*, 174–184. [CrossRef]
6. Tian, W.; Li, A.; Ren, X.; Josephine, Y. The threshold pressure gradient effect in the tight sandstone gas reservoirs with high water saturation. *Fuel* **2018**, *226*, 221–229. [CrossRef]
7. Morozov, P.; Abdullin, A.; Khairullin, M. An analytical model of SAGD process considering the effect of threshold pressure gradient. *IOP Conf. Ser. Earth Environ. Sci.* **2018**, *155*, 012001. [CrossRef]
8. Li, C. Is a starting pressure gradient necessary for flow in porous media? *Acta Petrol. Sin.* **2010**, *31*, 867–870.
9. Hansbo, S. Consolidation equation valid for both Darcian and non-Darcian flow. *Geotech* **2001**, *51*, 51–54. [CrossRef]
10. Swartzendruber, D. Modification of Darcy's law for the flow of water in soils. *Soil Sci.* **1962**, *93*, 22–29. [CrossRef]
11. Liu, H.H.; Birkholzer, J. On the relationship between water flux and hydraulic gradient for unsaturated and saturated clay. *J. Hydrol.* **2012**, *475*, 242–247. [CrossRef]
12. Liu, H.H. Non-Darcian flow in low-permeability media: Key issues related to geological disposal of high-level nuclear waste in shale formations. *Hydrogeol. J.* **2014**, *22*, 1525–1534. [CrossRef]
13. Wang, R.; Zhou, H.W.; Zhong, J.C.; Yi, H.; Chen, C.; Zhao, Y. The study on non-Darcy seepage equation of low velocity flow. *Sci. Sin. Phys.* **2017**, *47*, 064702. (In Chinese) [CrossRef]
14. Yang, S.; Wang, L.; Zhang, S. Conformable derivative: Application to non-Darcian flow in low-permeability porous media. *Appl. Math. Lett.* **2018**, *79*, 105–110. [CrossRef]
15. Zhou, H.W.; Yang, S.; Zhang, S.Q. Conformable derivative approach to anomalous diffusion. *Physica A* **2018**, *491*, 1001–1013. [CrossRef]
16. Zhang, H.J.; Jeng, D.S.; Barry, D.A.; Seymour, B.R.; Li, L. Solute transport in nearly saturated porous media under landfill clay liners: A finite deformation approach. *J. Hydrol.* **2013**, *479*, 189–199. [CrossRef]
17. Srinivasacharya, D.; Srinivasacharyulu, N.; Odelu, O. Flow and heat transfer of couple stress fluid in a porous channel with expanding and contracting walls. *Int. Commun. Heat Mass Transf.* **2009**, *36*, 180–185. [CrossRef]
18. Neto, L.B.; Kotousov, A.; Bedrikovetsky, P. Elastic properties of porous media in the vicinity of the percolation limit. *J. Pet. Sci. Eng.* **2011**, *78*, 328–333. [CrossRef]
19. Mokni, N.; Olivella, S.; Li, X.; Smets, S.; Valcke, E. Deformation induced by dissolution of salts in porous media. *Phys. Chem. Earth Parts A/B/C* **2008**, *33*, S436–S443. [CrossRef]
20. Gangi, A.F. Variation of whole and fractured porous rock permeability with confining pressure. *Int. J. Rock Mech. Min. Sci. Geomech. Abstr.* **1978**, *15*, 249–257. [CrossRef]
21. Archer, R.A. Impact of stress sensitive permeability on production data analysis. In Proceedings of the SPE Unconventional Reservoirs Conference, Keystone, CO, USA, 10–12 January 2008. SPE-114166-MS.
22. Schreyer-Bennethum, L. Theory of flow and deformation of swelling porous materials at the macroscale. *Comput. Geotech.* **2007**, *34*, 267–278. [CrossRef]
23. Jennings, J.B.; Carroll, H.B.; Raible, C.J. The relationship of permeability to confining pressure in low permeability rock. In Proceedings of the SPE/DOE Low Permeability Gas Reservoirs Symposium, Denver, CO, USA, 27–29 May 1981; p. SPE-9870-MS.
24. Tan, X.H.; Li, X.P.; Liu, J.Y.; Zhang, L.H.; Fan, Z. Study of the effects of stress sensitivity on the permeability and porosity of fractal porous media. *Phys. Lett. A* **2015**, *379*, 2458–2465. [CrossRef]
25. Khalil, R.; Al Horani, M.; Yousef, A.; Sababheh, M. A new definition of fractional derivative. *J. Comput. Appl. Math.* **2014**, *264*, 65–70. [CrossRef]
26. Abdeljawad, T. On conformable fractional calculus. *J. Comput. Appl. Math.* **2015**, *279*, 57–66. [CrossRef]

27. Zhao, D.; Luo, M. General conformable fractional derivative and its physical interpretation. *Calcolo* **2017**, *54*, 903–917. [CrossRef]
28. Lei, G.; Dong, Z.; Li, W.; Wen, Q.; Wang, C. Theoretical study on stress sensitivity of fractal porous media with irreducible water. *Fractals* **2018**, *26*, 1850004. [CrossRef]
29. Lei, G.; Mo, S.; Dong, Z.; Wang, C.; Li, W. Theoretical and experimental study on stress-dependency of oil-water relative permeability in fractal porous media. *Fractals* **2018**, *26*, 1840010. [CrossRef]
30. Yu, B.; Li, J. Some fractal characters of porous media. *Fractals* **2001**, *9*, 365–372. [CrossRef]
31. Cai, J.; Yu, B.; Zou, M.; Luo, L. Fractal characterization of spontaneous co-current imbibition in porous media. *Energy Fuels* **2010**, *24*, 1860–1867. [CrossRef]
32. Lei, G.; Dong, P.; Wu, Z.; Mo, S.; Gai, S.; Zhao, C.; Liu, Z.K. A fractal model for the stress-dependent permeability and relative permeability in tight sandstones. *J. Can. Pet. Technol.* **2015**, *54*, 36–48. [CrossRef]
33. Cai, J.; Wei, W.; Hu, X.; Wood, D.A. Electrical conductivity models in saturated porous media: A review. *Earth Sci. Rev.* **2017**, *171*, 419–433. [CrossRef]
34. Sheng, M.; Li, G.; Tian, S.; Huang, Z.; Chen, L. A fractal permeability model for shale matrix with multi-scale porous structure. *Fractals* **2016**, *24*, 1650002. [CrossRef]
35. Lu, T.; Duan, Y.; Fang, Q.; Dai, X.; Wu, J. Analysis of fractional flow for transient two-phase flow in fractal porous medium. *Fractals* **2016**, *24*, 1650013. [CrossRef]
36. Prakash, K.; Sridharan, A.; Prasanna, H.S. Dominant parameters controlling the permeability of compacted fine-grained soils. *Indian Geotech. J.* **2016**, *46*, 408–414. [CrossRef]
37. Zhang, J.; Jiang, S.; Wang, Q.; Hou, Y.; Chen, Z. Critical hydraulic gradient of piping in sand. In Proceedings of the Twentieth International Offshore and Polar Engineering Conference, Beijing, China, 20–25 June 2010.